Optimized Creep–Hysteresis Model to Improve Center-of-Pressure Detection in Pressure-Sensitive Mats

Sergio Domínguez-Gimeno, Carlos Medrano-Sanchez, *Senior Member, IEEE*, Raul Igual-Catalan, and Inmaculada Plaza-Garcia, *Senior Member, IEEE*

***Abstract*—Pressure-sensitive mats (PSMs) have a wide variety of applications. They can be used to measure the center of pressure (CoP) when a person is standing. Measuring CoP is useful for several applications, such as human stability assessment or fall risk prediction. Low-cost PSMs can be manufactured using piezoresistive materials, such as Velostat, whose conductance depends on the pressure exerted. However, these low-cost materials often suffer from hysteresis and creep. These effects worsen CoP measurement. Therefore, correction of hysteresis and creep effects is required to improve it. In this study, a creep–hysteresis correction model is applied to quantify CoP displacements obtained with PSMs. The model to correct creep and hysteresis effects is optimized using the CoP measurements themselves. This is a novel approach to optimize the creep and hysteresis model for this application. This approach has been experimentally tested on three different PSMs, including a commercial mat. Several tests and comparisons with existing models were performed, resulting in an improvement in CoP measurement when the CoP-optimized creep–hysteresis correction model was applied.**

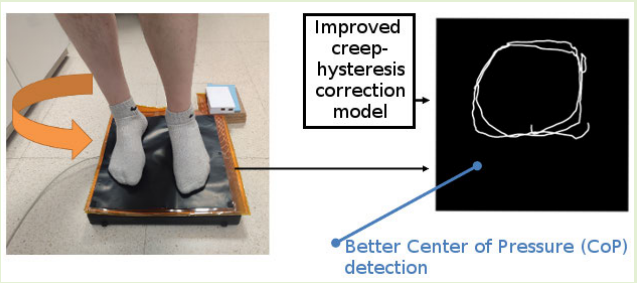

***Index Terms*— Center of pressure (CoP), creep, hysteresis, pressure-sensitive mat (PSM), resistive sensor array.**

I. Introduction

PRESSURE sensor arrays are 2-D arrangements of sensors that measure the pressure distribution over a surface. They have been used in several fields, such as aerospace, marine applications, robotics, sports, health, energy generation, and human–machine interface [1], [2], [3].

Received 25 February 2025; accepted 8 March 2025. Date of publication 18 March 2025; date of current version 1 May 2025. This work was supported in part by the Departamento de Educación, Ciencia y Universidades, del Gobierno de Aragón under Grant T49_23; in part by Ministerio de Ciencia, Innovación y Universidades (MCIN)/Agencia Estatal de Investigacion (AEI)/10.13039/501100011033 under Grant PID2021-125091OB-I00; in part by the European Regional Development Fund (ERDF) A way of making Europe; in part by the Spanish MCIN under Grant FPU20/04578; in part by the Spanish MCIN under Grant EST24/00517; and in part by the Universidad de Zaragoza, Fundación Ibercaja and Fundación CAI, under Grant IT 1/24. The associate editor coordinating the review of this article and approving it for publication was Prof. Mohammed Jalal Ahamed. *(Corresponding author: Sergio Domínguez-Gimeno.)*

This work involved human subjects or animals in its research. Approval of all ethical and experimental procedures and protocols was granted by the Corresponding Ethical Committee (Comité de Ética de la Investigación de la Comunidad Autónoma de Aragón - CEICA).

The authors are with the EduQTech Group, Escuela Universitaria Politécnica de Teruel, 44003 Teruel, Spain, and also with the IIS Aragón, University of Zaragoza, 50009 Zaragoza, Spain (e-mail: sdominguezg@unizar.es).

Digital Object Identifier 10.1109/JSEN.2025.3550826

Pressure sensor arrays can be integrated into flexible bases, obtaining pressure-sensitive mats (PSMs). PSMs have been used effectively in a variety of applications: electronic skins, sleeping assessment [4], posture studies [5], and human–machine interface systems [6], among others. The work of Cao et al. [7] presented a crosstalk-free interdigital electrode piezoresistive sensor matrix for automatic sitting posture recognition. They completely eliminated the crosstalk error, achieving accurate posture classification. Similarly, Bibbo et al. [8] presented textile pressure sensors to identify body posture variations during the performance of a stress-level test.

One common application of PSMs is the detection of the center of pressure (CoP). This is especially useful in health-related applications, like human fall risk assessment or gait quality studies, among others.

PSMs can be based on different sensing technologies, such as resistive, capacitive [9], triboelectric [3], piezoelectric, inductive [10], diode-based [11], or transistor-based [12]. The most common type of PSM is based on resistive sensor arrays. This type of PSM can be implemented with a continuous sheet of piezoresistive polymer embedded between electrode strips. Each piezoresistive material–electrode combination constitutes a pressure sensor of the array. Piezoresistive materials are often

influenced by temperature. In the work of Sundaram et al. [13], the Velostat[1] piezoresistive material was heated to various temperatures, resulting in changes in resistance values, especially above 60 °C. However, when the material was loaded [14], the resistance changes appeared at lower values. In addition, piezoresistive polymer sheets often exhibit nonidealities. These nonidealities make sensor modeling difficult and affect the accuracy of measurements recorded with the PSM. Two of the main nonidealities are hysteresis and creep.

On the one hand, in this article, hysteresis refers to a rate-independent memory effect. A piezoresistive material with hysteresis shows typical hysteresis loops in its resistance vs pressure curves [15]. On the other hand, the creep effect influences the resistance value of the material due to persistent mechanical stresses [16], [17]. Both effects are nonlinear, making their correction a challenge [18], [19], [20]. Several previous studies have taken these effects into account in PSMs, but they are rarely considered at the same time [16], [21].

This study aims to improve the measurement of CoP in PSMs. For that, a model to correct creep and hysteresis effects has been considered. This model has been optimized with the CoP measurements themselves, which is novel in this field. This novel solution has been compared with several reference approaches: the same model but characterized with experimental pressure–conductance measurements [22], a proportional model, models that only correct for one of the two effects (creep-only or hysteresis-only), a model based on conductance–pressure calibration curves [23], and a viscoelastic model [24]. Besides, the optimization has been carried out with only one subject performing a specific activity, while the resulting model can correct CoP in other subjects performing other activities. Moreover, three different PSMs, manufactured differently, have been considered in this article. The same type of model has been useful in all of them for CoP correction. Thus, this article shows a rather general way to improve PSM measurements by capturing a key aspect of sensor response. This is novel with respect to existing literature in this field [7], [8]. Furthermore, the effects of temperature on CoP detection using PSMs are addressed. To the best of our knowledge, this issue has not been discussed in depth in the literature.

The rest of this article is structured as follows: Section II presents the model to correct creep and hysteresis effects in PSMs based on the CoP measurements themselves. Section III presents the different PSMs studied in this work, as well as the force platform (FP) used to obtain the reference CoP measurements. Section IV describes the experimental setup of the study and the tests performed to record real CoP measurements from subjects. Section V presents the methods of the study to determine whether the optimized model improves CoP measurement in PSMs. Section VI presents the associated results. Section VII draws some conclusions. Appendix extends the article with some details about the importance of crosstalk correction when dealing with PSM measurements and its interplay with hysteresis and creep compensation.

[1]Registered trademark.

II. Theoretical Background

This section presents the optimized model to correct creep and hysteresis effects in PSMs and several existing models used for comparison.

A. Creep–Hysteresis Modeling

This model aims to correct creep and hysteresis phenomena in piezoceramic actuators [25], but can be applied to pressure-sensitive piezoresistive materials [22]. For the sake of clarity, the model and its parameters are briefly presented in this section. More detailed information can be found in [22]. However, the model parameters are found in a completely different way from a set of CoP measurements (see Section V-A), which is a novelty in this field.

1) Hysteresis Modeling: A modified Prandt–Ishlinskii model (MPI) is applied in this work to model the nonlinear hysteretic behavior of piezoresistive materials [25]. This model is based on one-side play (OSP) operators. Let $p(t)$ be a pressure signal for t in $[0, t_M]$. Assuming $p(t)$ is monotone in a set of subintervals $[t_i, t_{i+1}]$, with $0 < t_1 < t_2 < \cdots < t_M$, the OSP operator $F_r[p](t)$ gives an output $y_r(t)$, whose expression is (1). In this equation, r is the OSP threshold and $f_r(x, y)$ is obtained as shown in (2)

$$\begin{aligned} y_r(0) &= F_r[p](0) = f_r(p(0), 0) \\ y_r(t) &= F_r[p](t) = f_r\left(p(t), y_r(t_i)\right) \end{aligned} \tag{1}$$

$$f_r(x, y) = \max\left(x - r, \min\left(x, y\right)\right). \tag{2}$$

The output of the hysteresis model is a weighted sum of several OSPs $F_r[p](t)$, as seen in (3). To model the asymmetric hysteresis, a third-order polynomial is added to this weighted sum, whose coefficients are (a_1, a_2, a_3)

$$g_h(t) = a_1 p(t) + a_2 p^2(t) + a_3 p^3(t) + \sum_{i=1}^{N} b_i F_{r_i}[p](t) \tag{3}$$

where g_h represents the contribution of the hysteresis model to the sensor conductance. Six OSPs are considered in this work ($N = 6$) [22]. OSP weights are b_i and can be obtained with (4). As can be seen, weights follow an exponentially decreasing function. τ is the exponent that controls OSP weigths b_i, and ρ is its coefficient

$$b_i = \rho e^{-\tau r_i}. \tag{4}$$

2) Creep Modeling: If the creep effect is considered to be independent of the hysteresis, a creep operator can be easily modeled as a first-order linear time-invariant (LTI) model [19], [20]. The output of one single creep operator can be seen in (5). In this equation, $t_k = kT$, with T being the sampling period and l_i being the parameter that affects the decay of the exponential function. The global creep can be represented by a weighted sum of several creep operators, as seen in (6) [26], [27], [28]. The weights are w_i. In this work, two creep operators are taken ($N_C = 2$). Thus, the creep parameters that are considered are a set of two exponents (l_1, l_2) [(5)] and two weights of the creep

operator (w_1, w_2) [(6)]

$$y_{c,i}(t_k) = e^{-l_i T} y_{c,i}(t_{k-1}) + \left(1 - e^{-l_i T}\right) p(t_{k-1}) \quad (5)$$

$$g_c(t_k) = \sum_{i=1}^{N_c} w_i y_{c,i}(t_k) \quad (6)$$

where g_c represents the contribution of the creep model to the sensor conductance.

3) Combination of Hysteresis and Creep Modeling: The combination of hysteresis and creep is considered the sum of the above outputs. Thus, the final conductance is given by the sum of (3) and (6)

$$g(t) = g_h(t) + g_c(t). \quad (7)$$

4) Model Inversion and Model Indetermination: One of the advantages of the joint MPI and creep model is that the inverse model can be evaluated analytically. The details can be found in [22]. Schematically, if the direct model is written as $g = M(p)$, the inverse model allows obtaining the pressure from the measured conductance: $p = M^{-1}(g)$. Conventionally, the model is found from a set of measurements of the sensor response to a known applied pressure as done in [22]. However, in this article, the model parameters are found from a set of measurements of CoP displacements (see Section V-A) with a new objective function. This is a completely new way of obtaining them. The optimization of this objective function leads to different model parameters and better CoP estimation.

There is a side effect of the optimization proposed in Section V-A. Multiplying the pressure by a factor does not change the CoP displacements. Thus, the model is not completely determined because two models M_1 and M_2 such that $M_2^{-1}(g) \propto M_1^{-1}(g)$ would output the same CoP. Considering this indetermination, in this article, one of the parameters of the model has been set to a constant value $a_1 = 1.0$.

B. Other Models Used for Comparison

The optimized creep–hysteresis correction model presented in Section II-A has been compared with five existing models: proportional, creep-only, hysteresis-only, exponential calibration, and viscoelastic.

1) Proportional Model: A proportional model has been applied for comparison. This model assumes that the conductance of the piezoresistive material and the pressure exerted are proportional. It is the simplest model for piezoresistive materials since hysteresis and creep effects are neglected. Since the CoP trajectory is a relative measure, the exact value of the constant relating conductance and pressure is irrelevant and does not need to be found.

2) Creep-Only and Hysteresis-Only Models: Models that only consider hysteresis or creep are used. Following the notation in (7), the model that only considers hysteresis is represented in (8) and the model that only considers creep is represented in (9):

$$g(t) = g_h(t) \quad (8)$$

$$g(t) = g_c(t). \quad (9)$$

In this way, the influence of the combination of both effects can be analyzed.

3) Exponential Calibration Curves: Sygulla et al. [23] presented several pressure–conductance calibration models. These models allowed obtaining pressure from the conductance of a Velostat[1]-made sensor. The model that showed the smallest fitting error to the experimental data is given by (10), where p is the pressure and R is the sensor resistance. a, b, c, and d are the parameters of the model. In this case, they have been obtained in such a way as to minimize the error in CoP estimation (see Section V-A)

$$p(R) = a \cdot e^{b \cdot R} + c \cdot e^{d \cdot R}. \quad (10)$$

4) Viscoelastic Models: Another model for obtaining pressure from the conductance of a Velostat[1]-made sensor has also been considered for comparison. Vehec and Livovsky [24] presented a Velostat[1] model with a first-order system, which represents the viscoelastic behavior of the material. This approach is often used in creep compensation algorithms (see Section II-A.2). The sensor output is provided for a step function input pressure of magnitude p, as seen in (11). The output conductance g_{out} varies linearly with p through the constant k_p and also as a first-order system governed by k_e and τ. Since the pressure inputs in this study are not step functions, the transfer function of the first-order system must be obtained. After that, p can be obtained as a function of g. The way to adjust the model parameters is explained in Section V-A

$$g_{\text{out}}(t) = g_0 + p\left[k_p + k_e\left(1 - e^{-t/\tau}\right)\right]. \quad (11)$$

III. Instrument Description

In this study, three different piezoresistive PSMs are used to test the proposed model for CoP measurement. The piezoresistive PSMs exhibit nonidealities due to creep and hysteresis. All three PSMs have 16 rows and 16 columns (16-by-16 size), with an electrode size of 10 mm diameter each and covering a total area of 32 × 32 cm^2. The data acquisition system (DAQ) used to record PSM measurements has a sampling frequency of 100 Hz and exhibits crosstalk, as is usual in piezoresistive PSMs. This sampling frequency is high enough for gait and stability studies [29], [30], [31]. Records are sent via USB.

On the other hand, the gold-standard device used to obtain the true CoP measurements for comparison is an FP. An FP is a square-shaped reference system widely used in balance studies [32], [33], [34]. It is based on strain gauges in which creep and hysteresis effects are mostly negligible. An FP has only four sensing points located at the corners of the platform.

Sections III-A and III-B describe the PSMs and the reference FP used in this study.

A. Pressure-Sensitive Mats

1) *Interdigital PSM:* The structure of the interdigital PSM is depicted in Fig. 1 (left). The PSM electrodes are in the same plane as the piezoresistive sensing material, a continuous sheet of Velostat,[1] attached to them. The current flows only through the surface of the piezoresistive material in parallel to the electrode plane. The interdigital PSM has been developed by the authors of this study.

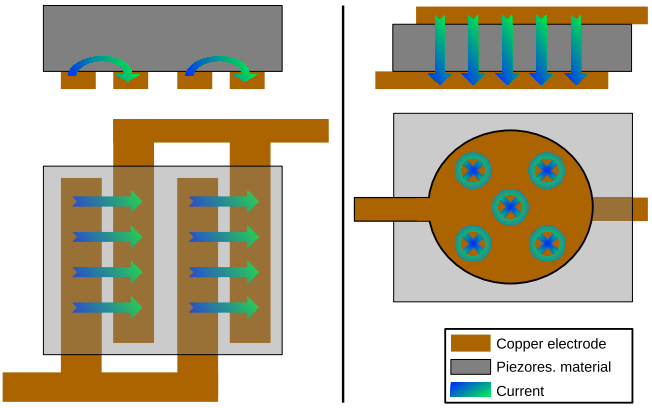

Fig. 1. Representation of the interdigital PSM (left) and the plain PSM (right).

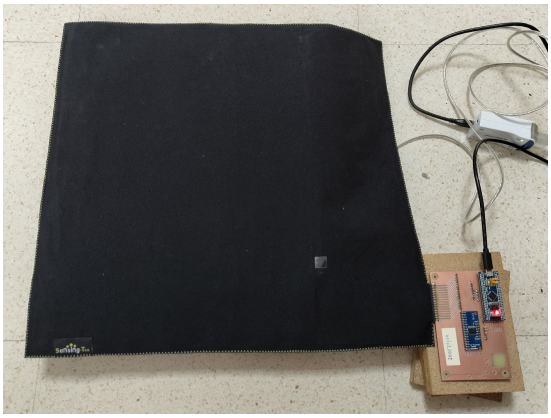

Fig. 2. Experimental setup. The selected PSM is placed on top of the FP and aligned with it.

2) *Plain PSM:* The structure of this PSM is depicted in Fig. 1 (right). This PSM has a sandwich-like structure in which the piezoresistive material, Velostat,[1] is placed between two parallel layers of electrodes. The current flows from one layer to the other in a perpendicular direction, passing through the piezoresistive material. The plain PSM has also been developed by the authors of this study.
3) *Commercial PSM:* The commercial PSM *Seating Mat* from Sensing Tex, Software Development Kit 05 with *Sensing Mat Demo Software v1.5.4*, is also used in this study [35]. This PSM is based on textile technology and electronic ink. It consists of a crossbar matrix of sensors of 16-by-16 size, similar to the plain PSM [35]. The commercial system includes a data acquisition card that records measurements and sends them to a computer via USB or Bluetooth. It also includes a software package that performs some crosstalk compensation. However, the same DAQ and measurement processing method (Section IV-C) used in this study for the other two PSMs can also be applied to this commercial PSM.

B. Force Platform

The reference FP used in this study is the PS-2141 PASPORT by Pasco [36]. This FP is a highly reliable gold standard for measuring forces applied on the platform. It can be configured to directly measure the CoP of a person standing on it.

For the experiments performed (Section IV), the CoP trajectories measured with the PSMs should be as close as possible to those provided by the reference FP.

IV. Experiments With Volunteers

To test whether the proposed CoP self-adjusting creep–hysteresis model improves CoP measurement in PSMs, different experiments have been carried out with volunteers.

A. Experimental Setup

The experimental setup developed involved both the PSMs and the reference FP. The reference FP was the base platform and the different PSMs were placed on top of it (separately, one at a time, so that three experimental setups were obtained). The FP and each selected PSM were closely aligned (Fig. 2). These two force-sensing systems were used to simultaneously record CoP measurements from different subjects performing a range of stability-related activities. The FP was configured to directly provide the (x, y) coordinates of the CoP with a sampling rate of 500 Hz. Each selected PSM simultaneously recorded its conductance matrix. Since PSMs are 16-by-16 in size, they also provide 16-by-16 conductance matrices. Each conductance matrix is called a frame. A new frame was recorded every 10 ms, so the PSM sampling rate was 100 Hz.

B. Experiments Performed

Different experiments were performed in the experimental setup with volunteers. Four subjects (ages between 24 and 51 years; weights between 56 and 82 kg; heights between 1.70 and 1.78 m) participated in the tests. All of them were informed of the purpose of the study and signed a written consent. The protocol of the experiments was approved by the corresponding ethical committee (Comité de Ética de la Investigación de la Comunidad Autónoma de Aragón - CEICA). The experiments consisted of performing different stability-related activities on the experimental setup as follows.

1) *Rotation:* The subject, standing in the experimental setup, performed circular movements with his/her body without releasing his/her feet from the surface of the setup. Neither the speed nor the amplitude of the rotation was imposed. The rotational movement was carried out uninterruptedly from 45 s to 1 min. If, during the activity, the subject lost balance, the experiment was repeated.
2) *Single-Legged (With the Right Leg):* The subject stood in the experimental setup on his/her right leg only. This activity was performed uninterruptedly from 45 s to 1 min. Again, if the balance was lost, the experiment was repeated.
3) *Single-Legged (With the Left Leg):* This activity was the same but using the left leg.

For each subject, the activities were repeated three times for each PSM-FP experimental setup. Between repetitions,

subjects were allowed to rest for 1 min. As the tests were performed for three different PSMs, a total of 27 activities per subject were recorded (9 per PSM-FP experimental setup).

C. Preprocessing of PSM Measurements

The reference FP directly provided the CoP (x and y), so no further processing was required. However, the PSMs provided a set of frames (16-by-16 conductance matrices). To obtain the CoP measurements (in the form of x and y coordinates) from the frames, the following preprocessing steps were performed.

1) *Filtering and Crosstalk Removal:* High-frequency noise was removed from the conductance matrices. In addition, the crosstalk effect was also eliminated using an effective fixed-point algorithm designed for that purpose [37], [38]. Crosstalk is a major problem in resistive sensor arrays [37], [39], [40], [41], [42]. Details on the crosstalk effect and its influence on creep–hysteresis analysis are given in Appendix . All the results shown in this work were obtained after crosstalk correction.
2) *Frame Rotation:* Frames from the PSMs were rotated so that their associated CoPs aligned with those provided by the reference FP. The specific rotation to be applied depends on the manufacturing process of the selected PSM. It may include 90° rotation and/or flips in the x- and y-axes.
3) *CoP Calculation:* For each frame of the selected PSM, the associated CoP (x and y coordinates) were obtained. Since the sampling rate of the PSMs (100 Hz) is five times lower than the sampling rate of the reference FP (500 Hz), the FP CoP measurements were decimated to match the PSM's sampling rate.
4) *CoP Synchronization and Signal Segmentation:* CoP measurements recorded with both the PSMs and the reference FP were temporally aligned using cross correlation of the x- and y-axes. Then, a 30-s window was extracted for each activity and repetition. Finally, for each axis, its mean value was subtracted so that the 30-s windows contained only relative displacements.

V. Methods

This section presents the different experiments and analyses performed to test the proposed model to correct creep and hysteresis effects optimized with the CoP measurements themselves. Its influence on the measurement of CoPs in the PSMs has been evaluated. The experiments are structured as follows.

1) As a prior step, the model for each PSM is optimized with the CoP measurements themselves. The optimization only takes into account one type of trial from a single subject to show the generalization capacity of the model.
2) Second, the error in CoP measurement using the optimized model is obtained for three different PSMs, including a commercial mat. The error includes an analysis of the whole set of experiments with subjects. The CoP measurement error is also obtained for the five existing models used for comparison, which were presented in Section II-B.
3) Then, the error in CoP measurement using the optimized model is compared with that obtained using a reference state-of-the-art model to correct creep and hysteresis effects adjusted with a pneumatic device.
4) Subsequently, CoP measurement is performed in the commercial PSM using both the proposed model and the commercial software and DAQ hardware provided by the manufacturer. The error in CoP measurement is compared.
5) Finally, the influence of temperature on CoP measurement is analyzed.

To calculate errors, CoP measurements from the reference FP have been used. The FP provides accurate measurements.

A. Optimized Creep–Hysteresis Correction Model

The correction model for creep and hysteresis effects applied to CoP measurement in PSMs has been optimized with the CoP measurements themselves. Specifically, the optimized creep–hysteresis model parameters were shown in Section II. For that, the simultaneous CoP measurements of the three PSMs (separately) and the reference FP were used. The lock-step Euclidean distance [Eu, (12)] was the figure of merit used to determine how well the CoP measurements in PSMs obtained with the creep–hysteresis model matched the true CoP measurements obtained with the FP. In the Eu equation, d_i is the Euclidean distance between two paired CoP measurements (the one provided by the selected PSM using the optimized model and the one given by the reference FP) and N is the number of paired CoP measurements considered

$$\mathrm{Eu} = \frac{\sqrt{\sum_{i=1}^{N} d_i^2}}{N}. \tag{12}$$

To perform this parameter optimization, the simulated-annealing method [22], [43] was used. This is a stochastic random search method that iterates all parameters at once around a set of initial values [43]. This method to adjust the model parameters has shown good performance in other applications [22].

This optimization process has been carried out for each of the three PSMs. For each PSM, only CoP measurements from one subject and trial were used for this optimization. Then, this one-subject-trial optimized model was used in the rest of the tests (see Sections V-B–V-D), where CoP measurements from all subjects and trials were considered. This approach evaluates the generalization ability of the optimized model.

The same process was used to adjust the parameters of the models used for comparison (see Section II-B).

B. Influence of the Optimized Model on CoP Measurement

The influence of the optimized model on the correction of creep–hysteresis effects in CoP measurements of PSMs has been tested.

Tests have been performed for each of the three PSMs (interdigital, plain, and commercial). For each PSM, the records of all subjects who participated in the experiments and the three different activities performed by each subject

(rotation, left-legged, and right-legged) were considered. CoP measurements were obtained separately for all subjects and each activity using the optimized creep–hysteresis correction model.

For the sake of comparison, the same CoP measurements were also estimated using the five existing models introduced in Section II-B.

The Eu was calculated with respect to the reference CoP measurements provided by the gold-standard FP. The Eu was obtained for the optimized model and the five existing models used for comparison.

C. Comparison of the Optimized Model With a Reference Creep–Hysteresis Model Adjusted With a Pneumatic Device

A reference creep–hysteresis model adjusted with a pneumatic device was used for comparison. This model was published in [22]. The parameters of this state-of-the-art model were adjusted for the interdigital PSM using the conductance–pressure curve obtained experimentally with a pneumatic device. These pressure–conductance data can be found in the GitLab repository [44]. The conductance of the PSM was registered by exerting different pressure values on the PSM with the pneumatic device. As the pneumatic device has a limited operating area, only creep–hysteresis models for small PSMs can be characterized in this way. In addition, although different PSMs might have been manufactured in the same way, the values of the model parameters are affected by characteristics such as aging, the number of previous operating cycles, and the way of exerting pressure on the PSM. Therefore, a heuristic scaling factor in the conductance was introduced into the model to compensate for these effects and to obtain a pressure value compatible with the subject's weight. This model was found to work well in an experimental setup with subjects conducting different postures similar to those performed in this study. Eu of this model has been taken from [22, Fig. 8].

CoP measurement error (Eu) for the interdigital PSM has been compared between the CoP-self-optimized creep–hysteresis model presented in this study and the reference model optimized with a pneumatic device. The CoP measurement error has been compared for the experiments performed by all subjects, and also for each posture separately.

D. Model Performance in a Commercial PSM

A further comparison has been conducted to test the performance of the proposed CoP-self-optimized creep–hysteresis model. For this comparison, the commercial PSM has been considered. The CoP measurement error (Eu) has been calculated for this PSM using two approaches.

1) *Proposed Optimized Model:* Measurements recorded with the DAQ and experimental setup described in Section IV (100-Hz sampling rate, USB connection) and processed with the optimized model introduced in Section II were used to calculate the Eu.
2) *Software and DAQ Hardware Provided by the Manufacturer:* The same experiments described in Section IV were repeated but, this time, acquiring the measurements with the DAQ provided by the manufacturer of the commercial PSM. The measurements were also processed with the software provided by the manufacturer to obtain the CoP trajectories. The DAQ was found to sample the entire PSM at approximately 11 Hz. For comparison, data were interpolated to obtain measurements sampled at 100 Hz.

For each approach, the Eu has been calculated with respect to the reference measurements provided by the FP. The Eu has been obtained three times for each activity from one subject.

E. Effects of Temperature

All the experiments and analyses presented in Sections V-A–V-D were conducted at room temperature (around 24 °C). It corresponds to a laboratory environment and was kept constant.

However, it is also interesting to study the effect of temperature on measurement error. For that, the same experiments presented in Section IV-B were repeated with the same four volunteers but under two different temperature conditions: at laboratory temperature (24 °C) and at a colder ambient temperature (10 °C). The experiments were performed sequentially. The plain PSM was used in this test. A thermographic camera was used to check that the temperature remained constant during the experiments. As the subjects' feet were observed to slightly warm the PSM, short pauses were taken between experiments to keep the PSM temperature constant.

Then, to study the effect of temperature on the CoP measurement, the new CHM was refitted, on the one hand, with the measurements taken at 24 °C, and, on the other hand, with the measurements taken at 10 °C. The CoP proportional model was also applied to each set of measurements for comparison.

F. Notation for Figures

Table I presents the notation associated with the different models. This notation has been used in the figure legends of Section VI (results and discussion) for clarity.

VI. Results and Discussion

A. Results of the Optimized Creep–Hysteresis Correction Model

Table II shows the optimal values of the parameters of the creep–hysteresis correction model obtained for each PSM. Those parameter values showed the lowest error in CoP estimation when the model was fit with the CoP measurements themselves from one subject and one trial. The error (Eu) in CoP estimation is included in Table II.

In addition, just to visualize the effect on CoP measurement when the proposed model is applied, as an example, Fig. 3 represents the CoP trajectories in the interdigital PSM measured with the reference device (FP) and the CoP trajectories obtained with the proposed model. The CoP trajectories depicted in Fig. 3 are for the subject and trial used to optimize

TABLE I
NOTATION FOR THE MODELS. THESE ARE USED IN SECTION VI. EACH SUBSECTION ONLY USES THOSE MODELS REQUIRED BY THE EXPERIMENTS PERFORMED IN IT

Abbreviation	Comment
CHM	Proposed creep-hysteresis model optimized with CoP measurements.
Prop	Proportional model optimized using CoP measurements.
OC	Model that only corrects for the creep effect, optimized with CoP measurements.
OH	Model that only corrects for the hysteresis effect, optimized with CoP measurements.
Sygulla	Model based on a calibration curve proposed by Sygulla *et al.* [23], optimized with CoP measurements.
Vehec	Viscoelastic model proposed by Vehec *et al.* [24], optimized with CoP measurements.
PD-CHM-ID	Reference creep-hysteresis model whose parameters were adjusted with a pressure device (PD) for the interdigital (ID) PSM [22]. The data associated with those experiments can be found in [44]. Eu of this model is taken from Fig. 8 in [22].
FP	Force platform, reference device.

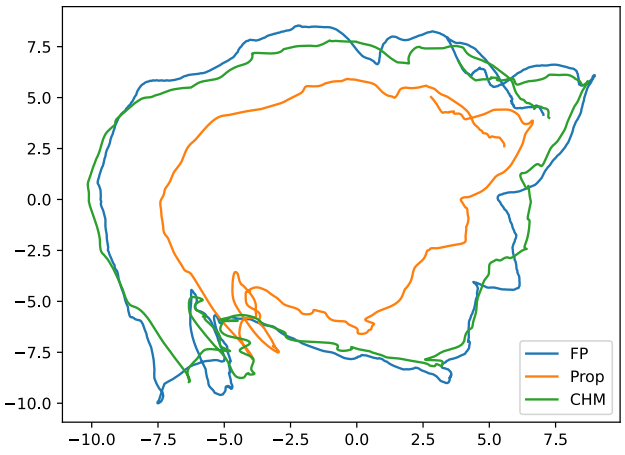

Fig. 3. CoP trajectories in the interdigital PSM obtained with the reference FP, the proportional model, and the optimized creep–hysteresis correction model. Legend notation is in Table I (only the required models and instruments are used in this figure).

the creep–hysteresis correction model. For comparative purposes, CoP trajectories for the same subject and trial when the proportional model is applied are also plotted. It can be seen that the CoP trajectories obtained with the proposed model are much closer to the real CoP trajectories than those obtained with the proportional model. Creep and hysteresis cause the CoP amplitude to decrease.

The PSM response time can be extracted from the obtained model parameters. The pair of values (l_1, l_2) are the inverse of the two constants of the creep model (as explained in Section II-A.2). Thus, the time constants are (11.1, 11.6 s) for the interdigital PSM, (13.0, 12.8 s) for the plain PSM, and (0.5, 6.6 s) for the commercial PSM. It is important to note that these response times do not affect CoP measurements after creep compensation.

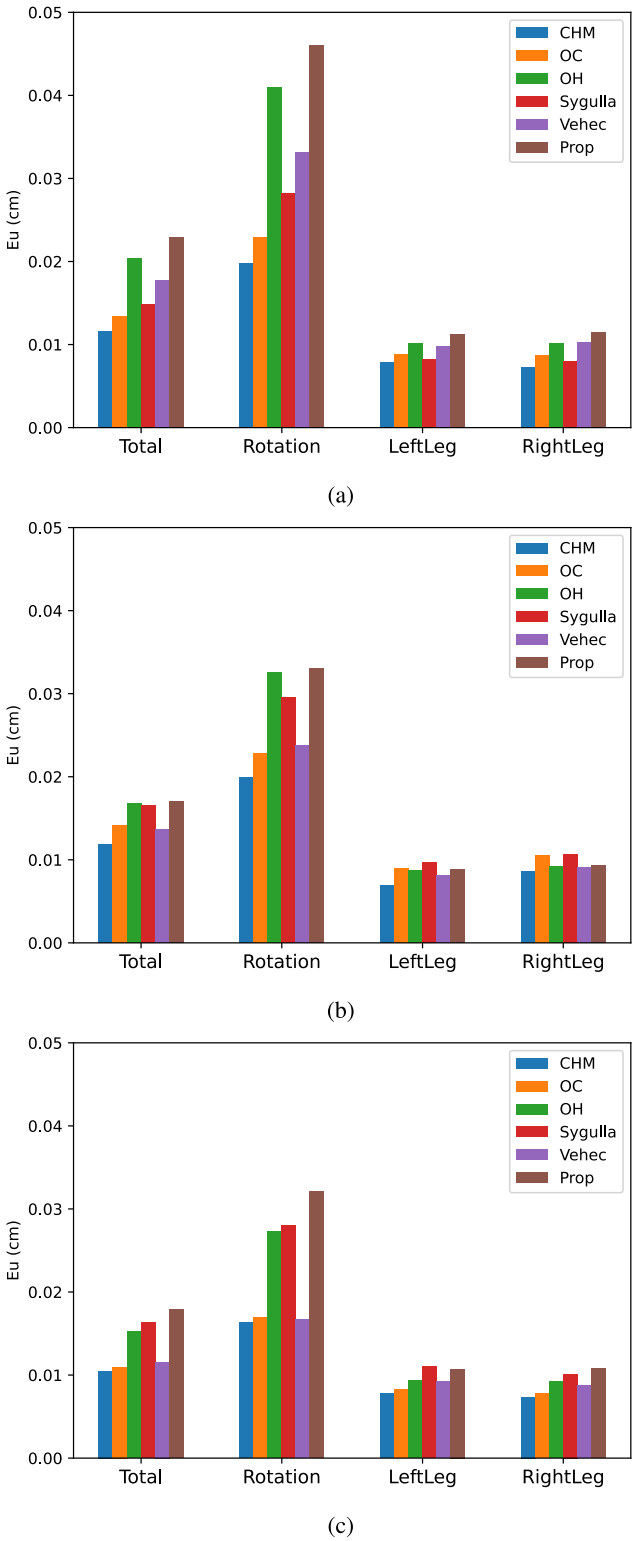

Fig. 4. Eu in CoP estimation for (a) interdigital PSM, (b) plain PSM, and (c) commercial PSM. For each PSM, models presented in Section II are used. Measurements from all subjects are considered. Legend notation is in Table I.

B. Results of the Influence of the Optimized Model on CoP Measurement

Fig. 4 shows the error (Eu) in CoP estimation for the three different PSMs for the proposed model to correct for

TABLE II
OPTIMAL VALUES OF THE PROPOSED CREEP–HYSTERESIS MODEL PARAMETERS FOR EACH PSM. THE ERROR VALUES CORRESPOND ONLY TO COP ESTIMATE FOR THE SUBJECT AND TRIAL USED IN THE PARAMETER SEARCH PROCESS

PSM	**Parameters values**									Eu **(cm)**
	Hysteresis					Creep				
	a_1	a_2	a_3	ρ	τ	l_1 (s^{-1})	l_2 (s^{-1})	w_1	w_2	
Interdigital	1	-238.7	1.92×10^4	0.312	887.4	0.0897	0.086	0.254	0.317	**0.01516**
Plain	1	1.129×10^4	-7.64×10^6	27.37	2845	0.0767	0.078	4.528	4.249	**0.01512**
Commercial	1	-1.310	-2.493×10^3	3.413	1.299	1.975	0.152	0.690	0.717	**0.00927**

the creep–hysteresis effects based on the CoP measurements themselves (blue bars). The same error metric is represented for the five models used for comparison: creep only (orange bars), hysteresis only (green bars), exponential calibration (Sygulla; red bars), viscoelastic (Vehec; purple bars), and proportional (brown bars). Results are shown for each trial separately (rotation, left leg, and right leg) considering all subjects, and also for all trials and subjects together.

It can be observed that the proposed creep–hysteresis correction model reduces the error for all PSMs and trials with respect to existing models. The proposed model improves CoP measurement in 24 of the 27 activities recorded in the experiments.

When the hysteresis-only model is applied, the error increases in all PSMs and activities. However, the creep-only model shows good performance in the commercial PSM [Fig. 4(c)]. It performs worse in the interdigital [Fig. 4(a)] and plain [Fig. 4(b)] PSMs, especially for single-legged activities. This suggests that, in these two PSMs, the creep-only model is unable to follow the rapid movements associated with the single-legged activities. The model based on exponential calibration curves ([23]) has a higher CoP estimation error than the optimized creep–hysteresis correction model. It shows the smallest error for the interdigital PSM. In contrast, the viscoelastic model ([24]) has a lower CoP estimation error in the plain and commercial PSMs. Its performance is similar to that of the creep-only model, which can be explained by the fact that the creep effect and the viscoelastic behavior can be represented by a first-order system transfer function. When the proportional model is applied, the interdigital PSM [Fig. 4(a)] shows a higher CoP measurement error than the plain and commercial PSMs (Fig. 4(b) and (c), respectively). However, the three PSMs behave similarly when corrected for creep and hysteresis effects with the proposed model. This indicates that the proposed model applies to different types of PSMs and has generalization capacity.

The best CoP measurement is obtained with the proposed creep–hysteresis correction model and the commercial PSM, followed by the plain PSM, and the interdigital PSM (blue bars of Fig. 4(a)–(c), respectively).

Fig. 4 also shows that the single-leg trials ("left leg" and "right leg") have a smaller CoP measurement error than the rotation trials for all models and PSMs. This can be explained as rotation experiments cover a wider measurement range. To fairly compare the creep–hysteresis correction regardless of the measurement range, the relative improvement in CoP measurement accuracy for the optimized creep–hysteresis model with respect to the proportional model has been calculated with (13). In this equation, Imp(%) is the relative improvement, Eu_{Prop} and Eu_{CHM} are the CoP measurement errors when the proportional and optimized creep–hysteresis models are applied, respectively. These relative improvements are shown in Table III. It can be seen that the optimized model corrects the CoP measurements to a greater extent in the rotation experiments. This indicates that rotational activities are more affected by creep and hysteresis. Thus, the optimized model is especially useful for rotation-dependent applications (such as fall-risk assessment [45])

$$\text{Imp}(\%) = 100 * \frac{|\text{Eu}_{\text{Prop}} - \text{Eu}_{\text{CHM}}|}{\text{Eu}_{\text{Prop}}}. \tag{13}$$

TABLE III
RELATIVE IMPROVEMENT (%) IN COP MEASUREMENT OF THE CREEP–HYSTERESIS MODEL WITH RESPECT TO THE PROPORTIONAL MODEL FOR EACH PSM. RELATIVE IMPROVEMENT IS OBTAINED FOR TWO ACTIVITIES (ROTATION AND SINGLE-LEGGED) IN ALL SUBJECTS

PSM	**Rotation**	**Single-legged**
Interdigital	57.0	33.2
Plain	39.6	14.9
Commercial	49.2	29.4
Average	48.6	25.8

C. Results of the Comparison of the Optimized Model With a Reference Creep–Hysteresis Model Adjusted With a Pneumatic Device

Fig. 5 shows the error in CoP measurement for the reference model adjusted with a pressure machine and for the proposed creep–hysteresis correction model. The values of the former approach were taken from [22]. It can be seen that the proposed model reduces the measurement error in all trials. These results indicate that the correction of the creep and hysteresis effects is more effective when the CoP measurements themselves are used for this purpose.

D. Results of Model Performance in a Commercial PSM

Table IV shows the CoP measurement error in the commercial PSM when using the commercial software and DAQ hardware provided by the manufacturer and when applying the proposed optimized model. It can be seen that the proposed model reduces the measurement error for all trials. The error

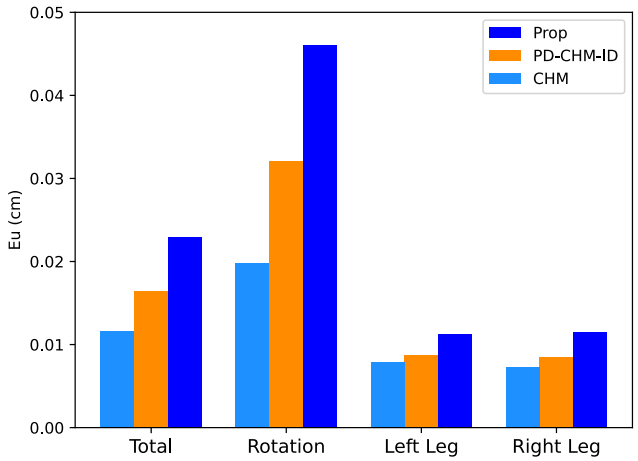

Fig. 5. Eu in CoP estimation for the interdigital PSM when creep and hysteresis effects are corrected with two different models (reference model based on a pneumatic machine, published in [22], and optimized model). Measurements from all subjects considered. The legend notation is in Table I.

TABLE IV
EU IN COP ESTIMATION FOR THE COMMERCIAL PSM USING THE COMMERCIAL DAQ AND SOFTWARE AND THE OPTIMIZED MODEL

System	All experiments	Rotation	Left Leg	Right Leg
Commercial	0.047	0.107	0.015	0.018
This work	0.010	0.016	0.008	0.007

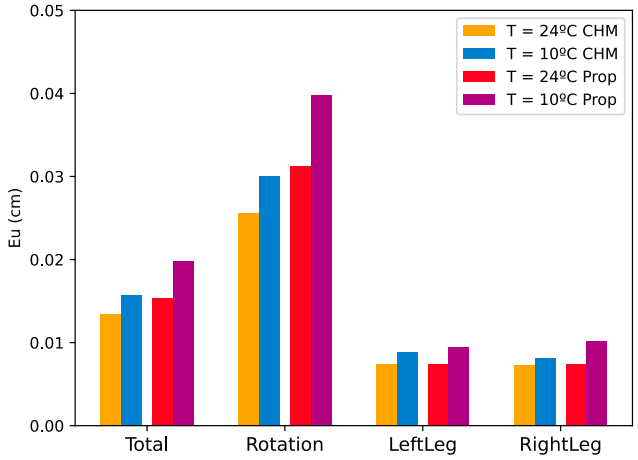

Fig. 6. Eu in CoP estimation for the plain PSM when the CoP is measured at the two temperatures studied (24 °C and 10 °C). Legend notation is in Table I.

reduction ranges from 46.7% in the "left leg" trials to 85% in the "rotation" trials. This can be explained because the commercial DAQ cannot maintain a constant sampling rate (around 11 Hz) and because the commercial software has neither creep–hysteresis error correction nor complete crosstalk removal.

The results show that the optimized creep–hysteresis correction model from the CoP measurements themselves is effective also in commercial PSMs when compared to the DAQ and software provided by the manufacturer.

E. Results of the Effects of Temperature

Fig. 6 presents the CoP measurement error values at different temperatures for the plain PSM. It can be seen that the error increases for the experiments performed at colder temperatures, both for the proportional model and for the CHM. Moreover, it is observed that creep–hysteresis parameters are temperature-dependent. One possible explanation for this phenomenon is that, when the material is colder, it is stiffer. This stiffness makes the piezoresistive material less sensitive to pressure, resulting in lower conductance variations.

VII. CONCLUSION

This study has shown that the accuracy of CoP measurements in PSMs improves when an optimized creep–hysteresis correction model is applied. For that, several experiments have been carried out with different subjects performing various CoP-related activities in different PSMs. The model was optimized with single-subject, single-activity CoP measurements. Then, the resulting model was used to correct creep–hysteresis effects in other subjects and activities, showing an improvement in CoP measurement accuracy. This demonstrates the generalization capacity of the optimized model, as it is independent of the specific subject.

Regarding the limitations of this study, it would be interesting to include more subjects of different weights and ages in the experiments. In fact, experiments involving more motion, such as rotation, are more affected by creep and hysteresis effects than those involving less motion. In addition, since few models combine the creep and hysteresis effects, the relationship between these two phenomena remains unclear. Future research may focus on new combined models that could be compared to the optimized model proposed in this study.

This study has also shown that mean CoP measurement accuracy improves for all PSMs. Thus, the optimized model does not depend on any specific PSM. Compared to existing models, the optimized model reduces measurement error in all PSMs. The same applies when compared to a creep–hysteresis correction based on the conductance–pressure curve obtained with a pressure machine. This can be explained by the fact that the optimized model is specifically oriented to the measurement of CoP. In relation to the limitations of the PSM study, it would be interesting to analyze the response to this creep–hysteresis model of other PSMs with different sizes and spatial resolutions.

When the optimized model and its associated DAQ are applied to a commercial PSM, an improvement in CoP measurement compared to the manufacturing results is also observed. This may be explained as the proposed system presents suitable creep–hysteresis correction, optimal sampling rate, and proper crosstalk correction [46] for CoP-related applications.

The effects of temperature on piezoresistive materials is a complex issue. The analysis performed shows that the creep–hysteresis parameters are temperature-dependent. However, due to the magnitude of the problem, further work will have to be done in the future.

Another future line of work is the improvement of the computation times of the entire system. The whole processing

TABLE V
AVERAGE EU IN COP ESTIMATION FOR ALL EXPERIMENTS AND VOLUNTEERS. FOUR COMBINATIONS ARE CONSIDERED: WITH AND WITHOUT CROSSTALK CORRECTION (*yC* AND *nC*, RESPECTIVELY), AND WITH AND WITHOUT CREEP–HYSTERESIS CORRECTION (*yH* AND *nH*, RESPECTIVELY)

	Method			
PSM	***nC-nH***	***yC-nH***	***nC-yH***	***yC-yH***
Interdigital	0.033	0.023	0.021	0.012
Plain	0.027	0.017	0.020	0.012
Commercial	0.028	0.018	0.022	0.010

system takes 382.1 s in total, of which 94.2% is for crosstalk compensation and the rest for CHM computation. Therefore, it is clear that crosstalk is the bottleneck. However, this may be suitable for many CoP-related applications, such as gait and stability analysis, since the data are usually postprocessed.

In conclusion, this study has presented a fairly general model for improving PSM measurements. The optimization strategy was based on capturing a key aspect of the response of the sensor array.

APPENDIX
THE CROSSTALK EFFECT

In this appendix, the effects of crosstalk on hysteresis and creep analysis are studied. First, the effects of crosstalk on PSM readout are addressed. Second, the effects of crosstalk on creep and hysteresis analysis are assessed.

On the one hand, Fig. 7 presents an experiment conducted to visualize the crosstalk effect in the commercial PSM. Fig. 7(a) depicts a schematic of the PSM with a person standing on it. Pressure is exerted on the yellow area (the volunteer's feet). The blue area remains unloaded (no pressure is exerted on it). Fig. 7(b) shows the conductance matrix acquired with the DAQ introduced in Section III. It presents crosstalk, as the silhouette of the foot is not well distinguishable. Moreover, it shows pressure values in the sensors corresponding to the blue area, which are unloaded in the mat. Therefore, they should not present conductance values associated with pressure. These measurement errors are due to crosstalk. In Fig. 7(c), the crosstalk effect is corrected by applying a fixed-point correction algorithm [37]. After crosstalk correction, the feet are better distinguishable, and, more importantly, the pressure values in the blue areas disappear. Ideally, the conductance in the blue regions should be zero, because the sensors behave like an open circuit in the absence of pressure.

The effect of crosstalk can be quantified. When crosstalk is not removed [Fig. 7(b)], the pressure within the blue regions represents 16.3% of the total conductance measured on the mat. When crosstalk is removed [Fig. 7(c)], this value represents only 0.95%. Thus, crosstalk removal is an essential step.

On the other hand, the influence of crosstalk on creep–hysteresis analysis is quantified. For that, Eu was obtained for the CHM model in all PSMs. Measurements registered in the experiments (Section IV-B) were used to calculate the Eu. The same measurements with and without crosstalk removal were considered for comparison. Table V presents the result of this analysis. Results show that crosstalk removal greatly decreases measurement error for all PSMs. Crosstalk is not an effect that can be compensated by fitting the CHM, because it occurs within each frame, while creep and hysteresis are time-dependent effects. It is also remarkable that creep–hysteresis correction is important even without crosstalk correction. When crosstalk is not removed, the percentage improvements in accuracy due to applying the CHM are 36.3%, 25.9%, and 21.4% for the interdigital, plain, and commercial PSMs, respectively. When crosstalk is corrected, the percentage improvements in accuracy due to applying the

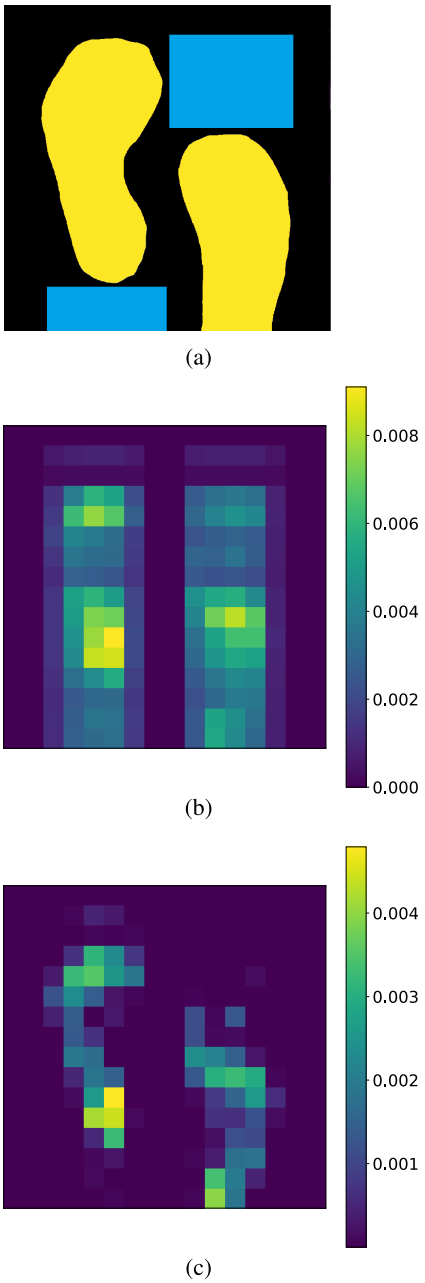

Fig. 7. Commercial mat capturing a person standing on the mat. (a) Feet positioned over the mat (yellow) and unloaded regions of interest (blue). (b) Conductance matrix before crosstalk removal. (c) Conductance matrix after crosstalk removal.

CHM are 47.8%, 29.4%, and 44.4% for the interdigital, plain, and commercial PSMs, respectively. Therefore, both crosstalk and creep–hysteresis compensations are required to obtain accurate CoP measurements in PSMs.

REFERENCES

[1] Y. S. Chong, K. H. Yeoh, P. L. Leow, and P. S. Chee, "Piezoresistive strain sensor array using polydimethylsiloxane-based conducting nanocomposites for electronic skin application," *Sensor Rev.*, vol. 38, no. 4, pp. 494–500, Sep. 2018.

[2] M. Chattopadhyay and D. Chowdhury, "Design and performance analysis of MEMS capacitive pressure sensor array for measurement of heart rate," *Microsyst. Technol.*, vol. 23, no. 9, pp. 4203–4209, Feb. 2016.

[3] A. Ahmed et al., "A washable, stretchable, and self-powered human-machine interfacing triboelectric nanogenerator for wireless communications and soft robotics pressure sensor arrays," *Extreme Mech. Lett.*, vol. 13, pp. 25–35, May 2017.

[4] A. K. M. Mahfuzul Islam et al., "Programmable neuron array based on a 2-transistor multiplier using organic floating-gate for intelligent sensors," *IEEE J. Emerg. Sel. Topics Circuits Syst.*, vol. 7, no. 1, pp. 81–91, Mar. 2017.

[5] H. Gleskova, A. A. Ishaku, T. Bednar, and R. Hudec, "Optimization of all-textile capacitive sensor array for smart chair," *IEEE Access*, vol. 10, pp. 48615–48621, 2022.

[6] S. Ji, J. Jang, J. C. Hwang, Y. Lee, J. Lee, and J. Park, "Amorphous oxide semiconductor transistors with air dielectrics for transparent and wearable pressure sensor arrays," *Adv. Mater. Technol.*, vol. 5, no. 2, Feb. 2020, Art. no. 1900928.

[7] Y. Cao et al., "A crosstalk-free interdigital electrode piezoresistive sensor matrix-based human-machine interaction system for automatic sitting posture recognition," *Sens. Actuators A, Phys.*, vol. 371, Jun. 2024, Art. no. 115284.

[8] D. Bibbo, M. Carli, S. Conforto, and F. Battisti, "A sitting posture monitoring instrument to assess different levels of cognitive engagement," *Sensors*, vol. 19, no. 3, p. 455, Jan. 2019.

[9] D. A. John, C. Parameswaran, S. Sandhu, and R. Dahiya, "Silk nanofibers-based soft and degradable capacitive pressure sensor arrays," *IEEE Sensors Lett.*, vol. 7, no. 5, pp. 1–4, May 2023.

[10] X. Tang, Y. Miao, X. Chen, and B. Nie, "A flexible and highly sensitive inductive pressure sensor array based on ferrite films," *Sensors*, vol. 19, no. 10, p. 2406, May 2019.

[11] H.-I. Yeom, J. Kim, G.-J. Jeon, J. Kim, and S. K. Park, "Active-matrix driven flexible pressure sensor array using oxide thin-film diode," *IEEE Electron Device Lett.*, vol. 44, no. 5, pp. 801–804, May 2023.

[12] X. Xue et al., "Flexible dual-parameter sensor array without coupling based on amorphous indium gallium zinc oxide thin film transistors," *Adv. Mater. Technol.*, vol. 7, no. 3, Mar. 2022, Art. no. 2100849.

[13] S. Sundaram, P. Kellnhofer, Y. Li, J.-Y. Zhu, A. Torralba, and W. Matusik, "Learning the signatures of the human grasp using a scalable tactile glove," *Nature*, vol. 569, no. 7758, pp. 698–702, May 2019.

[14] M. Hopkins, R. Vaidyanathan, and A. H. Mcgregor, "Examination of the performance characteristics of velostat as an in-socket pressure sensor," *IEEE Sensors J.*, vol. 20, no. 13, pp. 6992–7000, Jul. 2020.

[15] A. Visintin, *Differential Models of Hysteresis.*, vol. 111. Cham, Switzerland: Springer, 2010.

[16] A. Arndt, "Correction for sensor creep in the evaluation of long-term plantar pressure data," *J. Biomech.*, vol. 36, no. 12, pp. 1813–1817, 2003.

[17] S. Nizami, M. Cohen-McFarlane, J. R. Green, and R. Goubran, "Comparing metrological properties of pressure-sensitive mats for continuous patient monitoring," in *Proc. IEEE Sensors Appl. Symp. (SAS)*, Mar. 2017, pp. 1–6.

[18] Y. Peng, N. Yang, Q. Xu, Y. Dai, and Z. Wang, "Recent advances in flexible tactile sensors for intelligent systems," *Sensors*, vol. 21, no. 16, p. 5392, Aug. 2021.

[19] D. V. Sabarianand, P. Karthikeyan, and T. Muthuramalingam, "A review on control strategies for compensation of hysteresis and creep on piezoelectric actuators based micro systems," *Mech. Syst. Signal Process.*, vol. 140, Jun. 2020, Art. no. 106634.

[20] G.-Y. Gu, L.-M. Zhu, C.-Y. Su, H. Ding, and S. Fatikow, "Modeling and control of piezo-actuated nanopositioning stages: A survey," *IEEE Trans. Autom. Sci. Eng.*, vol. 13, no. 1, pp. 313–332, Jan. 2016.

[21] J. A. Sánchez-Durán, Ó. Oballe-Peinado, J. Castellanos-Ramos, and F. Vidal-Verdú, "Hysteresis correction of tactile sensor response with a generalized prandtl-ishlinskii model," *Microsyst. Technol.*, vol. 18, pp. 1127–1138, Apr. 2012.

[22] J. Martínez-Cesteros, C. Medrano-Sánchez, J. Castellanos-Ramos, J. A. Sánchez-Durán, and I. Plaza-García, "Creep and hysteresis compensation in pressure sensitive mats for improving center-of-pressure measurements," *IEEE Sensors J.*, vol. 23, no. 23, pp. 29585–29593, Dec. 2023.

[23] F. Sygulla, F. Ellensohn, A.-C. Hildebrandt, D. Wahrmann, and D. Rixen, "A flexible and low-cost tactile sensor for robotic applications," in *Proc. IEEE Int. Conf. Adv. Intell. Mechatronics (AIM)*, Jul. 2017, pp. 58–63.

[24] I. Vehec and L. Livovsky, "Flexible resistive sensor based on velostat," in *Proc. 43rd Int. Spring Seminar Electron. Technol. (ISSE)*, 2020, pp. 1–6.

[25] G.-Y. Gu, L.-M. Zhu, and C.-Y. Su, "Modeling and compensation of asymmetric hysteresis nonlinearity for piezoceramic actuators with a modified Prandtl–Ishlinskii model," *IEEE Trans. Ind. Electron.*, vol. 61, no. 3, pp. 1583–1595, Mar. 2014.

[26] P. Krejci and K. Kuhnen, "Inverse control of systems with hysteresis and creep," *IEE Proc.-Control Theory Appl.*, vol. 148, no. 3, pp. 185–192, May 2001.

[27] B. Mokaberi and A. A. G. Requicha, "Compensation of scanner creep and hysteresis for AFM nanomanipulation," *IEEE Trans. Autom. Sci. Eng.*, vol. 5, no. 2, pp. 197–206, Apr. 2008.

[28] Z. Sun, B. Song, N. Xi, R. Yang, L. Hao, and L. Chen, "Scan range adaptive hysteresis/creep hybrid compensator for AFM based nanomanipulations," in *Proc. Amer. Control Conf.*, Jun. 2014, pp. 1619–1624.

[29] T. K. Agrawal, S. Thomassey, C. Cochrane, G. Lemort, and V. Koncar, "Low-cost intelligent carpet system for footstep detection," *IEEE Sensors J.*, vol. 17, no. 13, pp. 4239–4247, Jul. 2017.

[30] J. A. Cantoral-Ceballos et al., "Intelligent carpet system, based on photonic guided-path tomography, for gait and balance monitoring in home environments," *IEEE Sensors J.*, vol. 15, no. 1, pp. 279–289, Jan. 2015.

[31] F. Quijoux et al., "A review of center of pressure (COP) variables to quantify standing balance in elderly people: Algorithms and open-access code*," *Physiological Rep.*, vol. 9, no. 22, Nov. 2021, Art. no. e15067.

[32] M. Piirtola and P. Era, "Force platform measurements as predictors of falls among older people—A review," *Gerontology*, vol. 52, no. 1, pp. 1–16, 2006.

[33] L. Walsh, B. R. Greene, D. McGrath, A. Burns, and B. Caulfield, "Development and validation of a clinic based balance assessment technology," in *Proc. Annu. Int. Conf. IEEE Eng. Med. Biol. Soc.*, Aug. 2011, pp. 1327–1330.

[34] J. Maciaszek, W. Osinski, R. Szeklicki, A. Salomon, and R. Stemplewski, "Body balance parameters established with closed and open eyes in young and elderly men," *Biol. Sport*, vol. 23, no. 2, p. 185, 2006.

[35] (2024). *Pressure Mat Dev Kit 2.0*. [Online]. Available: https://sensingtex.com/product/pressure-mat-dev-kit-2-0/

[36] PASCO. (2024). *Official Website of Pasco*. [Online]. Available: https://www.pasco.com/products/sensors/force/ps-2141

[37] C. Medrano-Sánchez, R. Igual-Catalán, V. H. Rodríguez-Ontiveros, and I. Plaza-García, "Circuit analysis of matrix-like resistor networks for eliminating crosstalk in pressure sensitive mats," *IEEE Sensors J.*, vol. 19, no. 18, pp. 8027–8036, Sep. 2019.

[38] J. Martinez-Cesteros, C. Medrano-Sanchez, I. Plaza-Garcia, and R. Igual-Catalan, "Uncertainty analysis in the inverse of equivalent conductance method for dealing with crosstalk in 2-D resistive sensor arrays," *IEEE Sensors J.*, vol. 22, no. 1, pp. 373–384, Jan. 2022.

[39] S. Domínguez-Gimeno, C. Medrano-Sánchez, R. Igual-Catalán, J. Martínez-Cesteros, and I. Plaza-García, "An optimization approach to eliminate crosstalk in zero-potential circuits for reading resistive sensor arrays," *IEEE Sensors J.*, vol. 23, no. 13, pp. 14215–14225, Jul. 2023.

[40] R. S. Saxena, N. K. Saini, and R. K. Bhan, "Analysis of crosstalk in networked arrays of resistive sensors," *IEEE Sensors J.*, vol. 11, no. 4, pp. 920–924, Apr. 2011.

[41] J. Wu, L. Wang, and J. Li, "Design and crosstalk error analysis of the circuit for the 2-D networked resistive sensor array," *IEEE Sensors J.*, vol. 15, no. 2, pp. 1020–1026, Feb. 2015.

[42] J. A. H. López, Ó. Oballe-Peinado, and J. A. Sánchez-Durán, "A proposal to eliminate the impact of crosstalk on resistive sensor array readouts," *IEEE Sensors J.*, vol. 20, no. 22, pp. 13461–13470, Nov. 2020.

[43] C. P. Robert, G. Casella, and G. Casella, *Monte Carlo Statistical Methods*, vol. 2. Cham, Switzerland: Springer, 1999.

[44] C. Medrano-Sanchez. (2023). *Creep_hyst_comp_psm. GitLab Repository*. Accessed: Feb. 24, 2025. [Online]. Available: https://gitlab.com/ctmedra1/cree_hyst_comp_psm/-/releases/v202310

[45] F. Quijoux et al., "Center of pressure displacement characteristics differentiate fall risk in older people: A systematic review with meta-analysis," *Ageing Res. Rev.*, vol. 62, Sep. 2020, Art. no. 101117.

[46] J. Martinez-Cesteros, C. Medrano-Sanchez, I. Plaza-Garcia, R. Igual-Catalan, and S. Albiol-Pérez, "A velostat-based pressure-sensitive mat for center-of-pressure measurements: A preliminary study," *Int. J. Environ. Res. Public Health*, vol. 18, no. 11, p. 5958, Jun. 2021.

Sergio Domínguez-Gimeno received the B.S. degree in electronic and automatic engineering and the M.S. degree in innovation and entrepreneurship in health and wellness technologies from the University of Zaragoza, Zaragoza, Spain, in 2020 and 2021, respectively, where he is currently pursuing the Ph.D. degree in electronic engineering with the EduQTech Research Group, Department of Electronic Engineering and Communications.

His research interests include crosstalk algorithms to increase accuracy in flexible pressure sensors, application of neural networks to pressure sensor arrays, and center-of-pressure detection using pressure-sensitive mats.

Carlos Medrano-Sanchez (Senior Member, IEEE) received the joint Ph.D. degree in physics from the University of Zaragoza, Zaragoza, Spain, and Joseph Fourier University, Grenoble, France, in 1997, and the Ph.D. degree from the Department of Electrical, Electronic and Control Engineering, Spanish University for Distance Education, Madrid, Spain, in 2015.

He is a Tenured Faculty Member with the Department of Electronic Engineering and Communications, University of Zaragoza, where he has been working since 1998. He has a broad research career, including topics, such as magnetism, data acquisition and control systems, and computer vision. He is the author of more than 40 articles in peer-reviewed journals. His current research interests include the fields of wearable sensors and pattern recognition for health and well-being applications.

Raul Igual-Catalan received the B.S. (Hons.) degree in telecommunications engineering-electronic systems and the M.S. degree in electronic engineering from the University of Zaragoza, Teruel, Spain, in 2008 and 2010, respectively, and the Ph.D. degree in electronic engineering from the University of Zaragoza (in international modality with stays at LIRMM, Montpellier, France), in 2014.

From 2013 to 2020, he was an Associate Professor with the University of Zaragoza, where he is currently a Tenured Faculty Member with the Electrical Engineering Department. He has participated in several regional, national, and international projects. His main research interests include the use of sensors for quality-of-life applications and the evaluation of power quality in renewable energy systems.

Inmaculada Plaza-Garcia (Senior Member, IEEE) received the degree in physics in 1994, the D.E.A. degree in design and manufacturing engineering, and the PhD. degree from the Department of Electronic Engineering and Communications, University of Zaragoza, Zaragoza, Spain, in 2001 and 2005, respectively.

She founded the Research Group EduQTech. She was the Dean of the Escuela Universitaria Politècnica de Teruel, Spain. She is now a Full Professor of electronic technology with the University of Zaragoza. She is the Director of the Institute of Studies of Teruel and the Director of the COGITIAR Chair. She has been the leader of 20 collaboration agreements and the main researcher of 27 projects (regional, national, and international) as well as the author of more than 100 works.

Dr. Plaza-Garcia has received numerous awards in research and management, some of them at international levels, for instance: the IEEE Education Society Chapter Achievement Award in 2011 as the Chairwoman of the Chapter and the 2011 Best Large Chapter Award-IEEE Region 8" as the Chairwoman. She was awarded the TAEE Association Award for the Professional Career in 2016 and the "Enterprising Woman 2018" from the University of Zaragoza. Finally, in 2023, she received the IEEE WIE Inspiring Member of the Year Award and the Tomás Pollán Award for multidisciplinary merit" in 2024. She is one of the founders of the IEEE Education Society Spanish Chapter, from which she was the Chairwoman from 2010 to 2012, and the TAEE Association (also the Chairwoman from 2022 to 2024).